

# RF TEST OF STANDING WAVE DEFLECTING CAVITY WITH MINIMIZED LEVEL OF ABERRATIONS

V. Paramonov\*, INR of the RAS, Moscow, Russia  
K. Floettmann, DESY, Hamburg, Germany

## Abstract

For diagnostics of longitudinal distribution of electrons in the unique REGAE bunches a specially developed deflecting structure with a minimized level of aberrations in the field distribution and improved RF efficiency is applied. A short deflecting cavity has been constructed and installed on the REGAE beam line. The cavity is tested at the operational level of RF power. The main distinctive features of the cavity are mentioned and the obtained results are reported.

## INTRODUCTION

The periodical Deflecting Structures (DSs) were introduced for charged particle deflection and separation. The bunch crosses the DS synchronously with the deflecting field  $E_d$ , which corresponds to the phase  $\phi = 0$  in the DS and all the particles get the similar increment in the transverse momentum  $p_t$ .

Now DSs find new applications in bunch rotation for the purpose of diagnostics of the longitudinal distribution, the emittance exchange and the luminosity improvements in colliders. For these applications a DS operates in another mode - the central particle of the bunch crosses the DS at a zero  $E_d$  value,  $\phi = 90^\circ$ . Downstream and upstream particles get opposite increments in  $p_t$ . In applications for bunch rotation a DS should produce the minimum possible own distortions in the original distributions of particles in the 6D phase space.

## METHODOLOGICAL AND PHYSICAL BASIS

The concept of DSs with a minimized level of own aberrations in  $E_d$  distribution, preferred for bunch rotation, was introduced in [1]. The equivalent deflecting field  $E_d$  is defined by transverse components of RF field as:

$$E_d = E_x - \beta Z_0 H_y, \quad Z_0 = \sqrt{\frac{\mu_0}{\epsilon_0}}, \quad (1)$$

where  $\beta$  is the relative velocity of particles. The reasons for the transverse emittance growth during bunch rotation are the aberrations - the nonlinear additives in the  $E_d$  distribution, which take place due to non relativistic energy of particles, additions from higher multipole modes and the higher spatial harmonics in the distribution of the dipole deflecting field. The analysis of the deflecting field distribution was performed [2] using the basis of hybrid waves  $HE$  and  $HM$  [3].

Both for travelling wave and standing wave DS operations, the deflecting field distribution can be represented [2] as an equivalent travelling wave. The main attention should be drawn to the higher spatial harmonics in  $E_d$  distribution [2, 4].

To estimate the level of higher spatial harmonics in  $E_d$  distribution and as a criterion for DS shape optimization parameters  $\delta\psi_j(z)$  and  $\Psi_j$  at the DS axis are introduced:

$$\delta\psi_d(z) = \psi_d(z) + \frac{\Theta_0 z}{d}, \quad \Psi_d = \max(|\delta\psi_d(z)|), \quad (2)$$

in the physical sense as the deviation and the maximal deviation in phase of the equivalent travelling wave  $E_d$  distribution from the synchronous harmonic. Here  $\Theta_0$  is the operating phase advance,  $d$  is the DS period length and  $\psi_d(z)$  is the phase distribution for the equivalent travelling  $E_d$  wave. During bunch deflection or bunch rotation, the central particle in the bunch sees the field:

$$E_{def}(z) = E_{d0} \cos(\psi_d(z)) \sim E_{d0} \left(1 - \frac{\Psi_d^2}{2}\right), \quad (3)$$

$$E_{rot}(z) = E_{d0} \sin(\psi_d(z)) \sim E_{d0} \Psi_d,$$

where  $E_{d0}$  is the deflecting field amplitude. With DS shape optimization we can change the ratio  $\frac{E_x}{Z_0 H_y}$  in  $E_d$  distribution, Eq. 1. Minimizing  $\Psi_d$  we keep the bunch close to the DS axis, where the nonlinear field of higher spatial harmonics is not large. Simultaneously the level of higher spatial harmonics in  $E_d$  will be reduced - the spatial harmonics in  $E_x$  compensate the spatial harmonics in  $Z_0 H_y$ . As a result, we have in orders smaller transverse emittance growth during bunch rotation [4].

For conventional DSs [3]  $\Psi_d$  minimization is an additional limitation and can be achieved only at the expense of reduction in the effective shunt impedance value  $Z_e$ . To combine the requirements for high RF efficiency and high field quality we need more freedom in the structure design. Based on promising parameters of the DS with a 'TE-like' operating mode [5] a decoupled DS was proposed with separated control on the RF efficiency and on the field quality. Possible solutions with decoupled DS are introduced in [6]. Later on the decoupled DS was investigated and optimized more thoroughly, showing very high rates in RF efficiency together with high field quality. A variety of possible attractive combinations in parameters of the developed DSs is described in [7].

## CAVITY DESIGN PARAMETERS

For implementation in the deflecting cavity for diagnostics of longitudinal particles distribution in the REGAE (Rela-

\* paramono@inr.ru

tivistic Electron Gun for Atomic Exploration) [8] a decoupled DSs option was selected as a compromise between RF parameters, low energy and other extreme beam parameters, reasonability in construction and a space available. The geometry of the decoupled DS, selected for implementations, is shown in Fig. 1. Operating in the standing wave mode, a

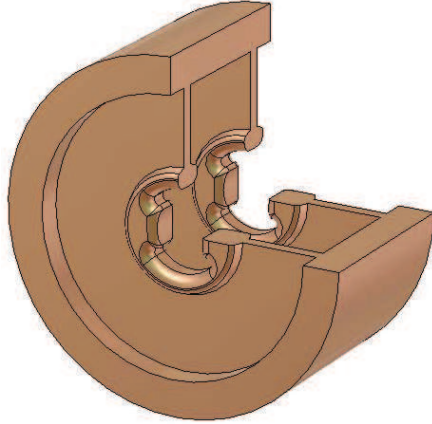


Figure 1: Geometry of the a decoupled structure, selected for deflecting cavity in the REGAE facility.

short cavity has three regular cells and two half cells at ends. The procedure for the end half cells formation is described, for example, in [6]. The main design parameters of the cavity are listed in Table 1. Figure 2 shows the distribution of

Table 1: Cavity Design Parameters

Parameter	Unit	Value
Operating frequency	MHz	2997.925
Energy of electrons	MeV	5
Operating phase advance	radian	$\pi$
Active cavity length	mm	$\approx 210$
Total cavity length	mm	270
Calculated quality factor		12550
Maximal phase deviation	radian	0.033
Separation with nearest mode	MHz	13.68
Effective shunt impedance, DS	$\frac{M\Omega}{m}$	43.2
Effective shunt impedance, cavity	$\frac{M\Omega}{m}$	7.58
Input RF power	kW	5
Expected deflecting voltage	kV	190

the effective deflecting field along the cavity axis, see Eq. 4, for bunch deflection (blue curve) and bunch rotation (red curve). As one can estimate from the red curve in Fig. 2, THE reduced oscillations of the bunch are expected for the bunch as a whole. The rms radius of the REGAE beam iN the place of deflecting cavity is expected to be  $\approx 0.5$  mm. Figure 3a depicts the surface for distribution of effective deflecting voltage  $\frac{V_d(x,y)}{V_d(0,0)}$  in the region  $-4 \text{ mm} \leq x, y \leq 4 \text{ mm}$  near the cavity axis. From the corresponding contour maps in Fig. 3b for deviation  $|\frac{V_d(x,y)-V_d(0,0)}{V_d(0,0)}|$  one can estimate  $V_d$  deviations as  $\leq \pm 0.5\%$  for the region  $-2 \text{ mm} \leq x, y \leq 2 \text{ mm}$

Technology

Beam diagnostics

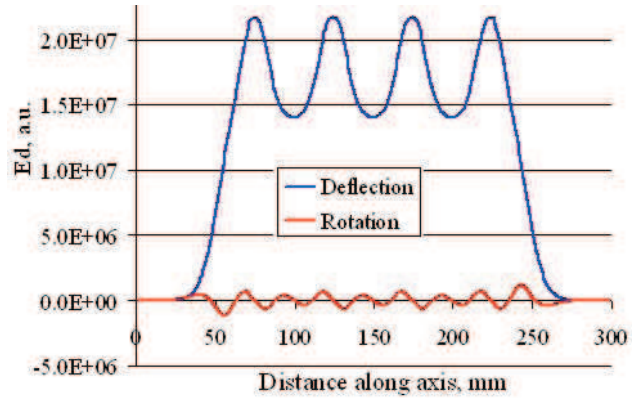


Figure 2: Distribution of the deflecting field  $E_d$  along the cavity axis for bunch deflection (blue curve) and bunch rotation (red curve).

and  $\leq \pm 1.0\%$  for the region  $-3 \text{ mm} \leq x, y \leq 3 \text{ mm}$ . The total beam is expected to be in a very linear deflecting field.

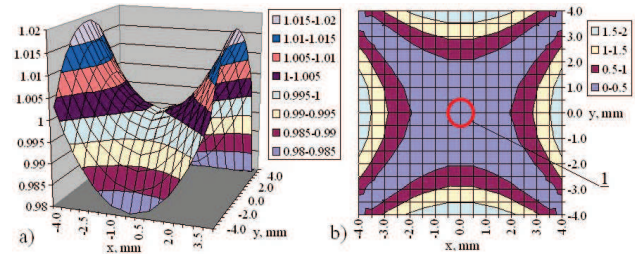


Figure 3: The surface of normalized value  $\frac{V_d(x,y)}{V_d(0,0)}$  (a) and contour map for normalized deviation  $|\frac{V_d(x,y)-V_d(0,0)}{V_d(0,0)}|$  near the cavity axis, 1 - rms diameter for the REGAE beam.

## CONSTRUCTION AND RF TUNING



Figure 4: Parts of the cavity after machining, CANDLE SRI.

Technical design of the cavity was developed and cavity parts with high precision and high quality of surface treatment, Fig. 4, were manufactured in CANDLE SRI, Yerevan, Armenia. After high temperature brazing with silver alloys in DESY the cavity was tuned to a frequency of 2997.91 MHz assuming vacuum conditions and operating temperature of  $35 \text{ C}^\circ$  [9]. The bead pull measurements showed

THPO079

following values of the transverse electric field component  $E_x$  100/100.08/100.04/99.86 in the middle points of irises. It indicates a very narrow spread in the cell frequencies and confirms high precision in cells dimensions.

## CAVITY AT THE REGAE BEAMLINE

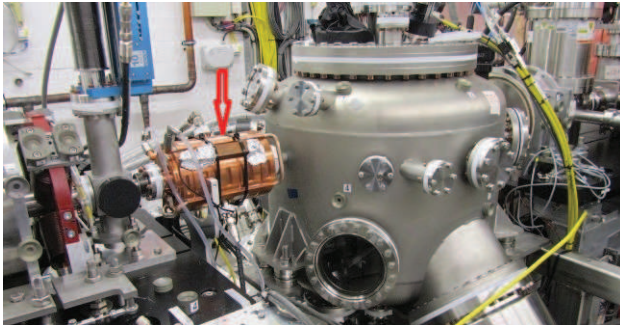


Figure 5: Cavity mounted at the REGAE beam line.

After RF tuning and vacuum test the inner cavity surface was cleaned according to cleaning procedure [10] and mounted at the REGAE beam-line, Fig. 5. The control over the operating frequency is carried out by the temperature of the water in the channels, adhered to the cavity body by heat conducting paste. The source of RF power supply is a solid-state amplifier with a nominal RF power of 5 kW. The input RF coupler is a loop, due to small dimensions produced by 3D printing and coated with a thin film of gold. By rotation a driving RF loop was matched to the reflection coefficient  $S_{11} = -31.6$  dB. The loaded quality factor  $Q_l$ , estimated from  $S_{11}$  measurements as  $Q_l = 4570$ , corresponds to the own quality factor  $Q_0 \approx 9150$ . The reasons for a moderate result in the obtained quality factor are under consideration. The transmission coefficient from driving to signal loops was adjusted to  $S_{12} = -37.1$  dB, ensuring sufficient power for RF diagnostics. RF power up to 5.5 kW was achieved in the cavity without any problem, Fig. 6. The cavity operates

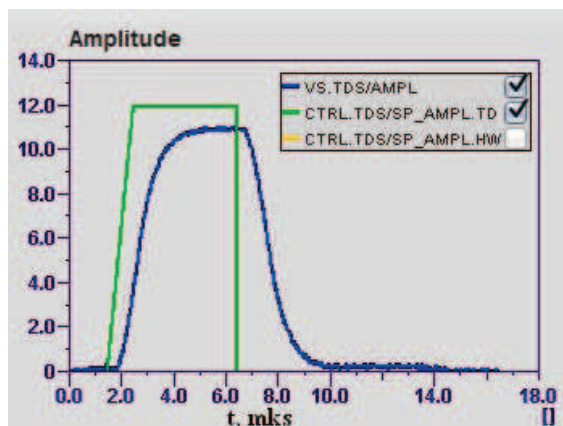


Figure 6: Envelopes of an output RF signal from the amplifier (green curve) and from RF probe in the cavity (blue curve).

with a very moderate value of deflecting field  $E_d \approx 0.9 \frac{MV}{m}$  and, correspondingly, rather low RF power. There were no indications or proofs for multipacting discharge during operation with nominal RF power.

## SUMMARY

For the first time a deflecting cavity specially optimized for minimal transverse emittance perturbation during rotation of a bunch was realized and RF tested. As compared to conventional deflecting structures, such z cavity provides physical benefits in applications for transformation of particle distributions in the bunch. These performances are requested in the facilities with unique bunch parameters. The successful test of the cavity at the nominal RF power was carried out. The cavity is ready for operation by purpose.

## ACKNOWLEDGEMENT

The authors are deeply grateful to the CANDLE SRI group for careful, accurate and high-quality manufacturing of cavity parts.

## REFERENCES

- [1] V. Paramonov, "Deflecting Structures with Minimized Level of Aberrations", in *Proc. Linac 2012*, Tel Aviv, Israel, September 2012, p. 445.
- [2] V. Paramonov, "Field distribution analysis in deflecting structures", DESY 18-13, DESY, arXiv:1302.5306v1, 2013.
- [3] H. Hahn, "Deflecting Mode in Circular Iris-Loaded Waveguides", *Rev. Sci. Inst.*, v. 34, n. 10, p. 1095, 1963.
- [4] K. Floettmann and V. Paramonov, "Beam dynamics in transverse deflecting rf structures", *Phys. Rev. ST Accel. Beams*, vol. 17, p. 024001, 2014.
- [5] V. Paramonov, L. Kravchuk and K. Floettmann, "RF Parameters of the TE - Type Deflecting Structure", in *Proc. Linac 2012*, Tel Aviv, Israel, September 2012, p. 366.
- [6] V. Paramonov, L. Kravchuk and K. Floettmann, "Standing Wave RF Deflectors with Reduced Aberrations", in *Proc. RuPAC 2012*, St. Peterburg, Russia, October 2012, p. 590.
- [7] V. Paramonov, "Effective RF deflecting structures for bunch rotation and deflection", in *Proc. RuPAC 2016*, St. Peterburg, Russia, November 2016, p. 201.
- [8] S. Manz et. al., "Mapping atomic motion with ultrabright electrons: towards fundamental limit in space time resolution", in *Faraday Discussion*, 177, p. 467-491, 2015, <http://dx.doi.org/10.1039/C4FD00204K>
- [9] V. Danielyan, K. Floettmann, V. Paramonov, A. Simonyan, V. Tsakanov, "Design, construction and tuning of an RF deflecting cavity for the REGAE facility", in *Journal of Physics: Conference Series*, to be published.
- [10] A. Brinkmann, J. Ziegler, "Dry-ice cleaning of RF-structures at DESY", in *Proc. Linac 2016*, East Lansing, September 2016, p. 52. doi : 10.18429/JACoW-LINAC2016-M00P05